# $SU(6)$ GUT origin of the TeV-scale vectorlike particles associated with the 750 GeV diphoton resonance

Bhaskar Dutta,[1] Yu Gao,[1] Tathagata Ghosh,[1] Ilia Gogoladze,[2] Tianjun Li,[3,4,5] and Joel W. Walker[6]

[1]*Department of Physics and Astronomy, Mitchell Institute for Fundamental Physics and Astronomy, Texas A&M University, College Station, Texas 77843-4242, USA*

[2]*Department of Physics and Astronomy, Bartol Research Institute, University of Delaware, Newark, Delaware 19716 USA*

[3]*Key Laboratory of Theoretical Physics and Kavli Institute for Theoretical Physics China (KITPC), Institute of Theoretical Physics, Chinese Academy of Sciences, Beijing 100190, People's Republic of China*

[4]*School of Physical Sciences, University of Chinese Academy of Sciences, Beijing 100049, People's Republic of China*

[5]*School of Physical Electronics, University of Electronic Science and Technology of China, Chengdu 610054, People's Republic of China*

[6]*Department of Physics, Sam Houston State University, Huntsville, Texas 77341, USA*

(Received 20 May 2016; published 22 August 2016)

We consider the $SU(6)$ grand unified theory (GUT) model as an explanation for the diphoton final state excess, where the masses of all associated particles are linked with a new symmetry breaking scale. In this model, the diphoton final states arise due to loops involving three pairs of new vectorlike particles having the same quantum numbers as down-type quarks and lepton doublets. These new vectorlike fermions are embedded alongside the standard model (SM) fermions into minimal anomaly-free representations of the $SU(6)$ gauge symmetry. The $SU(6)$ symmetry is broken to the standard model times $U(1)_X$ at the GUT scale, and masses for the vectorlike fermions arise at the TeV scale only after the residual $U(1)_X$ symmetry is broken. The vectorlike fermions do not acquire masses via breaking of the SM symmetry at the electroweak scale. The field which is responsible for the newly observed resonance belongs to the $\bar{6}_H$ representation. The dark matter arises from the SM singlet fermion residing in $\bar{6}$ and is of Majorana type. We explicitly demonstrate gauge coupling unification in this model, and also discuss the origin of neutrino masses. In addition to the diphoton final states, we make distinctive predictions for other final states which are likewise accessible to the ongoing LHC experimental effort.

DOI: 10.1103/PhysRevD.94.036006

## I. INTRODUCTION

Recently, both the ATLAS and CMS collaborations have reported an excess of events in the diphoton channel at a reconstructed invariant mass of about 750 GeV. This excess is visible in both the 13 TeV only [1,2] and $13+8$ TeV [3,4] LHC data analyses. The ATLAS collaboration reports a local signal significance of $3.9\sigma$ from an integrated luminosity of 3.2 $\text{fb}^{-1}$ at 13 TeV, and about $1.9\sigma$ from 20.3 $\text{fb}^{-1}$ of 8 TeV data. The CMS collaboration likewise reports a local signal significance of $3.4\sigma$ from combined luminosities of 3.3 and 19.7 $\text{fb}^{-1}$ at 13 and 8 TeV, respectively. CMS finds the observed significance to be maximized for a narrow decay width $\Gamma_S/M_S \lesssim 10^{-4}$, while the ATLAS data are reported to favor a larger width with $\Gamma_S/M_S \sim 0.06$. The collection of more data is necessary to clarify the status of the observed excess and the associated decay width.

A straightforward approach to explaining the diphoton excess is the introduction of a standard model (SM) singlet $S$ with a mass of 750 GeV accompanied by multiplets of vectorlike particles [5–7]. With vectorlike particles in the loops, the singlet $S$ can be produced via gluon fusion, and can likewise decay into a diphoton pair. The vectorlike particles can solve the vacuum stability problem [8].

In contrast to masses of the chiral fermions of the SM, the masses of the vectorlike quark and lepton are not tied to the electroweak scale, since they do not arise from the breakdown of the SM gauge symmetry. The natural question that arises is whether we may introduce a new symmetry that can be broken down at the TeV scale to generate masses for the vectorlike fermions. In this paper, we employ the gauge group $SU(6)$, placing the SM quarks, leptons and also the new vectorlike quarks and leptons into anomaly-free 15, $\bar{6}$ and $\bar{6}$ representations. $SU(6)$ is a subgroup of the anomaly-free exceptional group $E_6$, i.e., $E_6 \supset SU(6) \times SU(2)$, implying that our results may likewise be embedded within the context of an $E_6$ model. In our scenario, the $SU(6)$ gauge symmetry is broken down to $SU(3)_C \times SU(2)_L \times U(1)_Y \times U(1)_X$ at the grand unified theory (GUT) scale, and the residual $U(1)_X$ gauge symmetry is broken at the TeV scale by the vacuum expectation value (VEV) of SM singlets belonging to $\bar{6}_H$ and 21, producing vectorlike masses for three generations of new

 

down-type quarks and lepton doublets. The ratio of vectorlike quark and lepton masses $M_D/M_L$ gets fixed. The 750 GeV resonance arises from a scalar field which is the SM singlet within a $\bar{6}_H$ of $SU(6)$. The SM is subsequently broken at the weak scale. In addition to the new vectorlike quarks and leptons, the adoption of fundamental representations of $SU(6)$ also naturally implies two sets of SM singlets carrying the $X$ charge for each generation which develop Majorana masses ~TeV. One set of particles interacts with the SM leptons and is responsible for the lightness of the neutrino masses via a seesaw mechanism [9]. The lightest component of the second set is a dark matter (DM) candidate. We also investigate the gauge coupling unification in this model.

In Sec. II we detail the $SU(6)$ model and discuss the vectorlike particle masses, neutrinos, and DM. In Sec. III we discuss the gauge unification and GUT symmetry breaking. In Sec. IV we discuss the diphoton excess and predict cross sections for various other final states in the context of the $SU(6)$ model. In Sec. V we conclude.

## II. THE $SU(6)$ MODEL

In order to explain the observed excess of events around 750 GeV in the diphoton channel, we need to introduce new particles beyond the SM spectrum at a low scale. Particles with fermionic degrees of freedom are slightly better motivated than scalars, since their loop-induced contributions are larger, in general. Also, mass stability is much easier to explain in the fermionic case. It is very natural to ask about an underlying mechanism for the introduction of new vectorlike particles into the spectrum, and whether the necessary fields are an arbitrary choice or one governed by the enlarged symmetry structure of some GUT. In particular, we are interested in the question of what dynamics may protect the TeV-scale masses of these particles from GUT or Planck-scale corrections.

Whereas the SM fermions neatly fit into representations of $SU(5)$ or $SO(10)$, the minimal group structure which provides natural unification of the SM chiral fermions with additional particles transforming as vectorlike particles under the SM gauge symmetry is the $SU(6)$ GUT. The smallest anomaly-free set of chiral representations which fulfil this purpose (for one particle generation) in the $SU(6)$ GUT is

$$2 \times \bar{6} + 15. \tag{1}$$

The $\bar{6}$- and 15-dimensional representations decompose under the gauge symmetry as follows:

$$15 = (q, u^c, e^c) \oplus (\bar{L}_{15}(1,2,1/2), \bar{D}_{15}(3,1,-1/3)), \tag{2}$$

$$\bar{6} = (d^c, l) \oplus N', \tag{3}$$

$$\bar{6}' = (L_6(1,2,-1/2), D_6(\bar{3},1,1/3)) \oplus N. \tag{4}$$

Here we are using the common notation $q, u^c, e^c, d^c$, and $l$ for the SM fermions. $D_6$, $L_6$, $\bar{D}_{15}$, and $\bar{L}_{15}$ are vectorlike particles arising from $\bar{6}_i$ and $15_i$; $N$ and $N'_i$ are singlet fermions. For simplicity, we presently consider $d^c$ and $l$ to be elements of the $\bar{6}$ representation, while the new vectorlike particles are in $\bar{6}'$. However, as we elaborate later, the physical SM $d^c$ and $l$ actually arise from a superposition of $\bar{6}$ and $\bar{6}'$.

It is interesting to note that the additional vectorlike particles can only obtain mass once the rank of the $SU(6)$ gauge symmetry is broken. Specifically, the vectorlike particles are chiral under the residual $U(1)_X$ subgroup of $SU(6)$, and remain massless until this symmetry is broken. We consider the scenario where $SU(6)$ is broken at the GUT scale to $SU(3)_c \times SU(2)_L \times U(1)_Y \times U(1)_X$, and the $U(1)_X$ breaking scale is around a TeV. Thus, the $SU(6)$ GUT may facilitate a well-defined vectorlike particle spectrum with a common mass scale around a TeV. We emphasize that the new $U(1)_X$ symmetry breaking sector associated with this nonsupersymmetric extension of the standard model suffers from precisely the same issues of fine-tuning and hierarchy stabilization as the standard model electroweak symmetry breaking sector itself. Likewise, the scalar octet and triplet masses introduced at an intermediate scale (~$10^{10}$ GeV as in Table II) in order to facilitate gauge coupling unification (see Fig. 1) require very small (~$10^{-12}$) values of corresponding dimensionless Yukawa couplings in Table I.

The Yukawa sector in our model has the following form:

$$\mathcal{L} = 15 \cdot 15 \cdot 15_H + (\bar{6} + \bar{6}') \cdot 15 \cdot \bar{6}_H + \bar{6} \cdot \bar{6} \cdot 15_H + (\bar{6} + \bar{6}') \cdot 15 \cdot \bar{6}'_H + \text{H.c.} \tag{5}$$

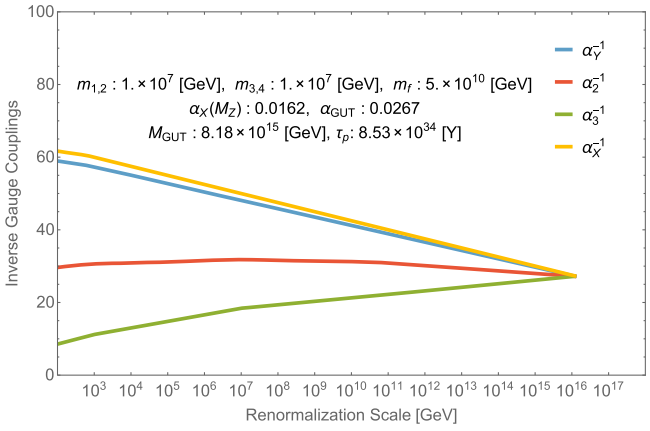


FIG. 1. Gauge coupling evolution with mass scales $m_{1,2} = m_{3,4} = 1 \times 10^8$ GeV for the adjoint triplet and octet scalars (two each) and $m_f = 2 \times 10^{10}$ GeV for a single fermionic weak triplet. Three pairs of vectorlike $(5, \bar{5})$ are additionally introduced, with a split mass hierarchy of 1 TeV and 600 GeV for the colored and noncolored field components, as well as a second Higgs doublet and a pair of light single scalars at 750 GeV. This corresponds to scenario $D$ of Table II.

TABLE I. The masses of physical scalar particles from the $\Phi_1$ and $\Phi_2$ adjoint multiplets after $SU(6)$ gauge symmetry breaking.

| $m_1^2$ | $m_2^2$ | $m_3^2$ | $m_4^2$ | $m_5^2$ | $m_6^2$ | $m_7^2$ | $m_8^2$ | $m_9^2$ | $m_{10}^2$ |
|---|---|---|---|---|---|---|---|---|---|
| $(8,1,0)_1$ | $(8,1,0)_2$ | $(1,3,0)_1$ | $(1,3,0)_2$ | $(3,1,1/3)$ | $(\bar{3},1,-1/3)$ | $(1,2,1/2)$ | $(1,2,-1/2)$ | $(3,2,5/6)$ | $(\bar{3},2,-5/6)$ |
| $2\lambda_2 V_1^2$ | $\frac{\lambda_5^2}{8\lambda_2} V_2^2$ | $2\lambda_2 V_1^2$ | $9\lambda_4 V_2^2$ | $(\lambda_6+\lambda_7)V_1^2$ | $(\lambda_6+\lambda_7)V_1^2$ | $4(\lambda_6+\lambda_7)V_2^2$ | $4(\lambda_6+\lambda_7)V_2^2$ | $M_{\rm GUT}$ | $M_{\rm GUT}$ |

TABLE II. Masses (in GeV) of the adjoint triplet and octet scalars (two each) and a single fermionic weak triplet for four benchmark unification scenarios. The resulting low-energy $U(1)_X$ coupling, grand unification scale (in GeV), and coupling, as well as the corresponding dimension-6 proton lifetime (in years), are also tabulated.

| Scenario | $m_{1,2}$ | $m_{3,4}$ | $m_f$ | $\alpha_X(M_Z)$ | $\alpha_{\rm GUT}$ | $M_{\rm GUT}$ | $\tau_p[{\rm Y}]$ |
|---|---|---|---|---|---|---|---|
| A | $1\times10^8$ | $1\times10^3$ | | 0.016 | 0.027 | $4\times10^{15}$ | $8\times10^{33}$ |
| B | $1\times10^{10}$ | $1\times10^{10}$ | $1\times10^{10}$ | 0.016 | 0.026 | $1\times10^{15}$ | $9\times10^{31}$ |
| C | $1\times10^4$ | $1\times10^4$ | $1\times10^{11}$ | 0.016 | 0.028 | $4\times10^{16}$ | $6\times10^{37}$ |
| D | $1\times10^7$ | $1\times10^7$ | $5\times10^{10}$ | 0.016 | 0.027 | $8\times10^{15}$ | $9\times10^{34}$ |

We have suppressed family and gauge indices for simplicity. In order to generate the SM fermion masses and mixing, as well as the vectorlike particle masses, we need to introduce the following $SU(6)$ representation for the Higgs field:

$$15_H + \bar{6}_H + \bar{6}'_H. \tag{6}$$

The up-type Higgs boson lives in $15_H$, the down-type Higgs lives in $\bar{6}_H$, and the SM singlet field which can break the extra $U(1)$ symmetry is in $\bar{6}'_H$. We need to introduce two different representations, i.e. $15_H + \bar{6}_H$, for the SM Higgs fields in order to have realistic quark and lepton masses. The reason for this is that taking only a single representation $\bar{6}_H$ (or $15_H$) leads to a nonrenormalizable coupling for one of the Yukawas [10]. For instance, the nonrenormalizable coupling in $15\cdot15\cdot\bar{6}_H\cdot\bar{6}'_H/M$ leads to a very small effective Yukawa coupling to the up-type quarks, since the singlet field responsible for $U(1)$ symmetry breaking takes a VEV at the TeV scale in our scenario.

The first term in Eq. (5) characterizes the up-type quark mass matrix and mixing. The second term does the same for the down-type quark and charged leptons. The assumption that $d^c$ and $l$ live only in the $\bar{6}$ representation implies $b-\tau$ Yukawa coupling unification at the GUT scale. This condition is problematic, since the $b$ and $\tau$ Yukawa couplings meet each other around $10^5$ GeV in the SM if we run under the renormalization group equations (RGEs) from low scale to high. However, considering instead that $d^c$ and $l$ are superpositions of $\bar{6}$ and $\bar{6}'$ breaks the $b-\tau$ Yukawa unification condition such that there is no conflict with experimental data. This mixing between the SM particles and the vectorlike particles is likewise helpful [11] to explain the Brookhaven National Laboratory muon $g-2$ data [12]. The third term in Eq. (5) provides for Dirac neutrino masses. The final term in Eq. (5) generates vectorlike masses for the new particles when the SM singlet component in $6'_H$ generates a VEV which breaks the $U(1)_X$ symmetry around the TeV scale, and moreover provides the scalar particle candidate ($S$) responsible for the observed 750 GeV resonance.

### Neutrino mass and dark matter

In order to avoid cosmological constraints on the number of degrees of freedom for massless particles [13], we need to generate a large mass for each of the $N$ and $N'$ fields, one of which we consider as a right-handed neutrino which interacts with the SM like $l$. The singlets $N$ and $N'$ can acquire Majorana mass from the interaction,

$$(\bar{6}\cdot\bar{6}+\bar{6}\cdot\bar{6}'+\bar{6}'\cdot\bar{6}')\cdot 21. \tag{7}$$

The 21-dimensional representation of $SU(6)$ contains single $S'$ under the SM gauge symmetry [14]. The VEV for this field is also associated with the TeV scale and can be responsible for breaking the $U(1)_X$ symmetry. $N'$ also interacts with $l$ and generates a Dirac mass, cf. Eq. (5). We thus have all the necessary ingredients for realization of a type-I seesaw mechanism for neutrino masses and mixing.

The lightest of the three generations of singlet Majorana type fields $N$ can be the DM candidate, if it is also lighter than $L$'s and $D$'s. In Ref. [15], a DM candidate of this type has been considered in the context of $SU(6)$, which is stabilized by an additional $Z_2$ discrete symmetry. We can stabilize the $N$ or $N'$ with an extra discrete symmetry like $Z_2$ in a scenario where the three families of fermions do not form three complete **27** representations, and some of the SM singlet fermion $N$ or $N'$ arises from a different **27**. This scenario, i.e. fermion multiplet splitting, can be realized in the orbifold GUTs or even in string models. In this case, $N$ or $N'$ can be the dark matter candidate after $U(1)_X$ gauge symmetry breaking [16].

## III. $SU(6)$ GUT SYMMETRY BREAKING AND GAUGE COUPLING UNIFICATION

As described previously, we are considering the symmetry breaking $SU(6) \to SU(3)_c \times SU(2)_L \times U(1)_Y \times U(1)$ at the GUT scale. In order to realize this process we require at least two scalar adjoint representations ($\Phi_1 + \Phi_2$) in the theory. For simplicity, we assume that $\Phi_1$ and $\Phi_2$ have a global $Z_2$ symmetry. In this case, the most general renormalizable potential involving only $\Phi_1$ and $\Phi_2$ has the following form:

$$\begin{aligned} V = & -\frac{M_1^2}{2}\mathrm{Tr}[\Phi_1^2] + \frac{\lambda_1}{4}\mathrm{Tr}[\Phi_1^2]^2 + \frac{\lambda_2}{4}\mathrm{Tr}[\Phi_1^4] - \frac{M_2^2}{2}\mathrm{Tr}[\Phi_2^2] \\ & + \frac{\lambda_3}{4}\mathrm{Tr}[\Phi_2^2]^2 + \frac{\lambda_4}{4}\mathrm{Tr}[\Phi_2^4] + \frac{\lambda_5}{2}\mathrm{Tr}[\Phi_1^2]\mathrm{Tr}[\Phi_2^2] \\ & + \frac{\lambda_6}{2}\mathrm{Tr}[\Phi_1\Phi_2]^2 + \frac{\lambda_7}{2}\mathrm{Tr}[\Phi_1^2\Phi_2^2]. \end{aligned} \tag{8}$$

For simplicity we further assume that $\lambda_6 \ll \lambda_i$ and $\lambda_7 \ll \lambda_i$ ($i \neq 6$ or 7). One possible VEV configuration of the $\Phi_1$ and $\Phi_2$ fields is

$$\Phi_1 = \mathrm{diag}(+1,+1,+1,-1,-1,-1) \times V_{\Phi_1}, \tag{9}$$

$$\Phi_2 = \mathrm{diag}(+1,+1,+1,-2,-2,+1) \times V_{\Phi_2}, \tag{10}$$

where

$$V_{\Phi_1}^2 = \frac{M_1^2(4\lambda_3+\lambda_4) - 4M_2^2\lambda_5}{(4\lambda_3+\lambda_4)(6\lambda_1+\lambda_2) - 24\lambda_5^2}, \tag{11}$$

$$V_{\Phi_2}^2 = \frac{6M_1^2\lambda_5 - M_2^2(6\lambda_1+\lambda_2)}{72\lambda_5^2 - 3(4\lambda_3+\lambda_4)(6\lambda_1+\lambda_2)}. \tag{12}$$

After GUT symmetry breaking, various components of the $\Phi_1$ and $\Phi_2$ scalar multiplets obtain different masses, as in Table I. At the low scale we also have vectorlike particles transforming under the SM gauge symmetry,

$$3 \times [(1,2,1/2) + (1,2,-1/2) + (3,1,-1/3) + (\bar{3},1,1/3)]. \tag{13}$$

These multiplets are from the fermionic $(15 + \bar{6})$ representations of the $SU(6)$ GUT, constituting full $5 + \bar{5}$-dimensional representations of the $SU(5)$ subgroup. As shown in Eq. (7), these vectorlike particles obtain a common mass once the $\bar{6}'$ field develops a VEV for its sixth element, breaking the additional $U(1)_X$ gauge symmetry. Since all vectorlike particles from Eq. (12) have the same mass, they do not change the relative slopes of RGE running for the gauge couplings at one-loop level and induce only a slight modification at two-loop level. So, as shown in Fig. 1, gauge coupling unification is obtained by a suitable choice of the $\lambda_1$ coupling, as reflected in the physical masses of the particles in Table I. In order to have a light Higgs doublet at the low scale, a fine-tuning procedure is required, as is characteristic of any nonsupersymmetric GUT.

We have studied the evolution of the $SU(3)_c \times SU(2)_L \times U(1)_Y \times U(1)$ gauge couplings under the renormalization group at the second loop, including leading feedback between the single loop evolution of the top, bottom and tau Yukawa couplings and the SM gauge sector. The details relevant to this analysis are presented in Appendix B. Broadly speaking, we may break the new fields introduced beyond the standard model fermions and light Higgs boson into two groups, labeled $I$ and $II$, which are active around the TeV scale, and above the intermediate ($\sim 10^{10}$ GeV) scale, respectively. The matter content in region $I$ consists of three generations of the fermionic fields described in Eq. (1), i.e. the vectorlike $3 \times (5, \bar{5})$ and the fermionic singlets $3 \times (N, N')$, plus additional scalars corresponding to a second electroweak Higgs doublet and two scalar SM singlets from the $\bar{6}$ and 21 representations. Masses for colored and noncolored components of the new vectorlike particles are fixed at 600 GeV and 1 TeV, respectively. This scale is favored by the diphoton analysis and this splitting is consistent with that suggested by running of the relevant Yukawa couplings under the renormalization group. Since the candidate for the diphoton resonance is included as one of the new scalars, we choose for simplicity to assign the new light scalars a common mass of 750 GeV. In region $II$, we activate two pairs each of scalars in the $SU(2)_L$ adjoint scalar triplet and $SU(3)$ adjoint scalar octet, as well as a single fermionic weak triplet. The generation of these scalar masses is described in Table I, and we carry over the notation $m_{1,2}$ and $m_{3,4}$ for the octet and triplet, respectively. We simplify to a common mass for each set, which may be interpreted as a geometric mean. The mass of the fermionic triplet is denoted as $m_f$.

Table II reports the induced low-energy value of the $U(1)_X$ coupling $\alpha_X(M_Z)$, the grand unified coupling $\alpha_{\mathrm{GUT}}$, and mass scale $M_{\mathrm{GUT}}$, as well as the corresponding dimension-6 proton lifetime $\tau_p$ for four examples of the renormalization group flow. The unification solution is not greatly affected by small variation of the vectorlike mass scale within the physical window, or even by omission of these fields (except for a reduction in $\alpha_{\mathrm{GUT}}$). Essentially similar results are obtained with the further mutual inclusion of one pair each of adjoint scalars carrying the quantum numbers of the right-handed down-quark conjugate and the left-handed lepton doublet at the intermediate scale. Near GUT-scale threshold corrections from scalar fragments, e.g. with quantum numbers of the quark doublet, likewise do little to alter the essential features described. The first selected scenario $A$ omits the fermionic adjoint triplet, while including one pair each of the octet and triplet scalar adjoints. It is found that the GUT unification scale is unacceptably light unless the triplet mass is quite low. Pushing $m_{3,4}$ all the way down to 1 TeV

sets an upper bound of $M_{\rm GUT} \lesssim 4 \times 10^{15}$ GeV for this field content. Triple unification is then achieved for $m_{1,2} \simeq 1 \times 10^8$ GeV. Scenario $B$ introduces additionally a single fermionic weak triplet, and imposes the constraint of degenerate mass scales $m_{1,2} = m_{3,4} = m_f$. It is found that strict unification near $1 \times 10^{15}$ GeV is induced if the new fields are placed at an intermediate scale, around $1 \times 10^{10}$ GeV. The GUT scale in each of the prior scenarios remains somewhat light, suggesting overly rapid decay of the proton, with a dimension-6 lifetime as low as the order of $10^{32}$ years. Given that the GUT scale varies inversely with the scalar adjoint mass, scenario $C$ is designed to investigate the maximal offset which may be achieved relative to the field content of scenario $B$. If the scalar masses are pushed down to around 10 TeV, then the unification scale moves up to around $4 \times 10^{16}$ GeV, extending proton decay beyond the reach of foreseeable experimental searches. However, it is not phenomenologically necessary to consider such an extreme splitting. Mild splitting between a minimal configuration of fields at the intermediate mass scale (with or without inclusion of near-GUT threshold corrections) is sufficient to acceptably elevate the unification scale. Scenario $D$ is selected to demonstrate such a physically suitable possibility, taking $m_{1,2} = m_{3,4} = 1 \times 10^7$ GeV and $m_f = 5 \times 10^{10}$ GeV, lifting the unification scale to around $8 \times 10^{15}$ GeV, and extending the proton lifetime to a safe yet testable range around $9 \times 10^{34}$ years. The scenario $D$ unification is depicted in Fig. 1. A stable prediction is made for the low-energy value of the $SU(6)$-normalized coupling $\alpha_X$. Given that the leading one-loop beta coefficient $b_4 = 403/60$ is very similar to that of the SM hypercharge [this is a rather generic feature of $U(1)'$ subgroups from $E_6$ embeddings reflecting the fact that the number of particles which do not form GUT multiplets is small], the slope of their running is almost degenerate, and a value $\alpha_X(M_Z) \simeq 0.016$ is to be expected at the $Z$-boson mass, or a value $\alpha_X(\text{TeV}) \simeq 0.017$ at the TeV scale.

We note that there are many other ways to likewise achieve gauge coupling unification in nonsupersymmetric theories [17]. For instance, one can use the split multiplet mechanism [18], which can explain why we have incomplete multiplets near the GUT scale and facilitate gauge coupling unification around $10^{16}$ GeV. We emphasize again that the $SU(6)$ gauge group can be embedded into $E_6$, deferring the details of a reinterpretation of our result in this framework to Appendix A.

## IV. THE DIPHOTON EXCESS

As described previously, the singlet $S$ of $\bar{6}'_H$ is presently considered to provide the scalar particle responsible for the observed 750 GeV resonance. $S$ is coupled to $L$ and $D$ via $\bar{6}' \cdot 15 \cdot \bar{6}'_H$, as shown in Eq. (5). We thereby get photon, $Z$, $W$, and jet final states.

The leading order decay rate of the resonance $S$ into various diboson final states is given by

$$\Gamma(S \to \gamma\gamma) = \frac{M_S^3}{64\pi}\left(\frac{e^2}{4\pi^2}\right)^2 \left| \sum_{f=D,L} N_f N_c^f Q_f^2 \lambda_f \left\{ \frac{1}{M_f} A_{\frac{1}{2}}(\tau_f) + \sum_{i=1}^{2} \frac{A_f}{2M_{\tilde{f}}^2} A_0(\tau_{\tilde{f}}) \right\} \right|^2,$$

$$\Gamma(S \to ZZ) = \frac{M_S^3}{64\pi}\left(\frac{1}{4\pi^2}\frac{g_2^2}{c_W^2}\right)^2 \left| \sum_{f=D,L} N_f N_c^f (T_3^f - Q_f s_W^2)^2 \lambda_f \left\{ \frac{1}{M_f} A_{\frac{1}{2}}(\tau_f) + \sum_{i=1}^{2} \frac{A_f}{2M_{\tilde{f}}^2} A_0(\tau_{\tilde{f}}) \right\} \right|^2 \times \left(1 - 4\frac{M_Z^2}{M_S^2} + 6\frac{M_Z^4}{M_S^4}\right)\sqrt{1 - 4\frac{M_Z^2}{M_S^2}},$$

$$\Gamma(S \to Z\gamma) = \frac{M_S^3}{32\pi}\left(\frac{1}{4\pi^2}\frac{e g_2}{c_W}\right)^2 \left| \sum_{f=D,L} N_f N_c^f Q_f (T_3^f - Q_f s_W^2) \lambda_f \left\{ \frac{1}{M_f} A_{\frac{1}{2}}(\tau_f) + \sum_{i=1}^{2} \frac{A_f}{2M_{\tilde{f}}^2} A_0(\tau_{\tilde{f}}) \right\} \right|^2 \left(1 - \frac{M_Z^2}{M_S^2}\right)^3,$$

$$\Gamma(S \to W^+W^-) = \frac{M_S^3}{32\pi}\left(\frac{1}{4\pi^2}\frac{g_2^2}{2}\right)^2 \left| \sum_{f=D,L} N_f N_c^f \lambda_f \left\{ \frac{1}{M_f} A_{\frac{1}{2}}(\tau_f) + \sum_{i=1}^{2} \frac{A_f}{2M_{\tilde{f}}^2} A_0(\tau_{\tilde{f}}) \right\} \right|^2 \left(1 - 4\frac{M_W^2}{M_S^2} + 6\frac{M_W^4}{M_S^4}\right)\sqrt{1 - 4\frac{M_W^2}{M_S^2}},$$

$$\Gamma(S \to gg) = \frac{M_S^3}{8\pi}\left(\frac{g_3^2}{4\pi^2}\right)^2 \left| \sum_{f=D} N_f T_r \lambda_f \left\{ \frac{1}{M_f} A_{\frac{1}{2}}(\tau_f) + \sum_{i=1}^{2} \frac{A_f}{2M_{\tilde{f}}^2} A_0(\tau_{\tilde{f}}) \right\} \right|^2, \tag{14}$$

where $N_f = 3$ is the number of copies of $(5, \bar{5})$, $N_c^f$, being the color factor, attains a value 3 (1) for $D(L)$, $\lambda_f$ are the Yukawa couplings of $f$ with $S$, $A_f$ are the trilinear couplings of $S$ with the supersymmetric partners of the vectorlike fermions, $f = D, L$, if we supersymmetrize our model. $Q_f$ and $T_3^f$ are the electric charge and third component of the isospin of fermions (and their superpartners whenever they are included in the calculation),

respectively. $\sin\theta_W$ ($\cos\theta_W$), where $\theta_W$ is the Weinberg angle, is denoted by $s_W$ ($c_W$) in the above equations. The Dynkin index for color triplet $D$, $T_r = 1/2$, is used in the $\Gamma(S \to gg)$ calculation. Finally the loop functions for spin-1/2 and spin-0 particles are given by

$$A_{\frac{1}{2}}(\tau_f) = 2\int_0^1 dx \int_0^{1-x} dz \frac{1-4xz}{1-xz\tau_f},$$
$$A_0(\tau_{\tilde{f}}) = \int_0^1 dx \int_0^{1-x} dz \frac{4xz}{1-xz\tau_{\tilde{f}}}, \quad (15)$$

with $\tau_i = \frac{M_S^2}{M_i^2}$. Please note that in the decay width calculations involving massive gauge bosons, the effect of gauge boson mass on loop functions has been neglected since they change the loop functions only by ∼5%. In addition we also assumed that the mixing between the sparticles ($\tilde{f}_i$, $i = 1, 2$) is negligible in the formulas of Eq. (14).

A pair of isosinglet $D$-type quarks can be strongly produced at the LHC and studied in the $H/Zb+$ anything or $Wt+$ anything channels. The current strongest ATLAS bound on $D$-type vectorlike quark masses of $\lesssim$800 GeV arises from the dilepton final state when the $D$ predominantly decays to $Wt$. However, the bound relaxes to $\lesssim$650 GeV if the dominant decay mode is $Hb$ (see [19] and references therein). The particular branching ratios (BRs) for a benchmark point (BP) depend on the mixing of $D$ with SM down-type quarks and we can tune the mixing parameters to satisfy the bounds. In contrast, the vectorlike leptons $L$ are less likely to be produced at the LHC since they do not necessarily have large mixings with SM leptons. Hence, they can easily evade the excited lepton searches by CMS [20].

We have performed a separate evolution of the $\lambda$ couplings of vectorlike fermions in the $3 \times (5, \bar{5})$ representations between the GUT scale and the scale of the observed resonance $M_S \sim 750$ GeV, finding attraction toward a fixed point in the vicinity of $\lambda_L = 0.4$ and $\lambda_D = 0.7$ that is essentially similar to the result obtained in our previous analysis [21] in the context of a pure $SU(5)$ supersymmetric GUT. Additional details are provided in Appendix B. We therefore select benchmark masses for the $L$ and $D$ which are broadly consistent with this prediction, noting that the specific values do not have a significant impact on the gauge unification. $M_D$ and $M_L$ masses arise due to the VEV of the SM singlet component $\bar{6}'_H$. The $Z'$ mass associated with the $U(1)_X$, however, arises from the largest VEV of the SM singlet components of $\bar{6}'_H$, $\bar{6}_H$ and 21 which is around a TeV.

The diphoton production cross-section at the LHC, assuming the narrow-width approximation, can be written as

$$\sigma_{\gamma\gamma} = \frac{K\pi^2}{8M_S}\frac{\Gamma(S \to gg)\Gamma(S \to \gamma\gamma)}{\Gamma_S} \times \frac{1}{s}\int dx_1 dx_2 f_g(x_1) f_g(x_2)\delta\left(x_1x_2 - \frac{M_S^2}{s}\right), \quad (16)$$

where $\sqrt{s} = 13$ TeV, $K$ is the QCD K-factor, $x$ denotes the fraction of each beam's energy carried away by the corresponding gluon, and $f_g$ is the gluon parton distribution function (PDF) inside a proton. The total decay width of $S$ is denoted by $\Gamma_S = \Gamma_{\gamma\gamma} + \Gamma_{Z\gamma} + \Gamma_{ZZ} + \Gamma_{WW} + \Gamma_{gg}$. We have used the PDFs of `MSTW2008LO` [22] for the gluon luminosity calculation with the factorization scale set at $M_S$. We evaluated $\alpha_s$ to be 0.092 at our scale of interest but we found that $\alpha$ does not change significantly from its value (0.0078) at $M_Z$. A K-factor of 2.5 is used in our calculation, which is the K-factor for 750 GeV SM-like Higgs bosons [23]. We also included the $\alpha_s^4$ correction to $\Gamma_{gg}$, which increases it by a factor of ∼1.7 [24].

We note that the CMS and ATLAS collaboration results disagree to some extent on the experimentally observed width of the resonance. While ATLAS obtains the highest significance for a large width of $\Gamma_S/M_S = 0.06$, CMS data are fitted better by the narrow width of $\Gamma_S/M_S = 1.4 \times 10^{-4}$. However, the data collected so far are insufficient to support either case convincingly. The loop-induced diphoton and dijet widths are inadequate to account for the $\mathcal{O}(10)$ GeV width required by ATLAS. Reference [25] has recently performed a likelihood analysis to fit 8 and 13 TeV data sets of both CMS and ATLAS experiments. Interestingly, inclusion of the 8 TeV data lowers the best-fit cross section by a factor ∼2 and shifts the resonance to ∼745 GeV. These authors further noticed that a narrow-width explanation of the excess reduces the combined significance from 3.9 to 3.3$\sigma$. Finally, they conclude that a narrow-width resonance between ∼730 and 755 GeV can be fit by $\sigma_{\gamma\gamma} \sim$ 1–5 fb at the 2$\sigma$ level (with the best fit being at 2.6 fb).

In the left panel of Fig. 2 we present $\sigma_{\gamma\gamma}$ contours that fit the data, for different values $M_L$ and $M_D$ belonging to generic $3 \times (5, \bar{5})$ models. This figure clearly shows that the data can be fit for a range of values of $M_L$ and $M_D$. The reader should note that the points belonging to the $SU(6)$ model under discussion are a subset of the generic $3 \times (5, \bar{5})$ points shown in the left panel. In our $SU(6)$ model $M_L/M_D = \lambda_L/\lambda_D$ is enforced since both $L$ and $D$ masses are generated by the $U(1)_X$ breaking VEV. The points belonging to the $SU(6)$ model are shown by the black dashed line. In the right panel of Fig. 2, we show the cross section times branching ratio of $S$ into various diboson channels as a function of the mass of $L$, keeping $M_D$ fixed at $M_L\lambda_D/\lambda_L$ as required by our $SU(6)$ model. Evidently, the excess can be fit for $M_L \lesssim 500$ GeV. For this range of $M_L$ values, the cross sections in associated diboson channels are within current experimental limits. We discuss the strongest of those limits in the subsequent paragraphs.

In Table III, we report the values of cross sections in different channels along with the total decay width for two BPs belonging to $3 \times (5, \bar{5})$, setting $M_L/M_D = \lambda_L/\lambda_D$ as required by our $SU(6)$ model. BP-1 and BP-2 respectively

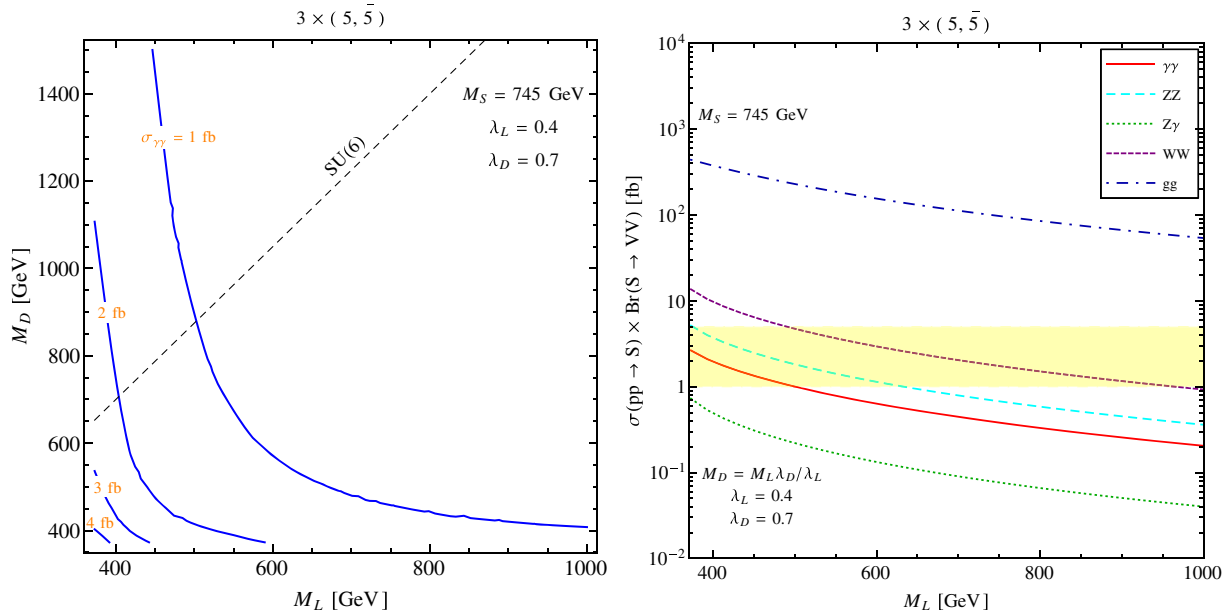


FIG. 2. (Left panel) The contours of $M_L$ and $M_D$ that fit $\sigma_{\gamma\gamma} = 1$–5 fb for $M_S = 745$ GeV. The black dashed line corresponds to points belonging to the $SU(6)$ model under discussion. (Right panel) The corresponding cross sections of $S$ decaying to various diboson channels as a function of $M_L$ with $M_D = M_L\lambda_D/\lambda_L$ as required by our $SU(6)$ model. The yellow shaded region shows the allowed values of $\sigma_{\gamma\gamma}$ for a narrow-width resonance. $\lambda_L$ and $\lambda_D$ are set to 0.4 and 0.7, respectively, for both plots.

correspond to the best-fit and $2\sigma$ lower limit of $\sigma_{\gamma\gamma}$ needed for a narrow-width resonance. Since the best-fit $\sigma_{\gamma\gamma}$ is achieved for $M_L \approx M_S/2$, we cannot fit the $2\sigma$ upper limit of it without introducing tree-level decay of $S$ into a pair of $L$. We note that using $M_L$ values of 374 and 500 GeV for BP-1 and BP-2, respectively, in the table above, the ratio of the corresponding diphoton production cross sections is 2.61, which is different from just $(500/374)^2 = 1.79$ due to the $M_L$ dependence of the loop functions. In addition, since $M_D$ values of BP-1 and BP-2 are not too high, their effect in this ratio cannot be neglected either. The results presented in Table III using decay width expressions of Eq. (14) agree with the numbers obtained from analytical expressions given in Refs. [5,6]. The adoption of three copies of $(5, \bar{5})$ vectorlike matter is well motivated in a GUT context such as $E_6 \supset SU(6)$, where the generations of new particles are in one-to-one correspondence with the SM generations. Clearly, from Table III and Fig. 2, $3 \times (5, \bar{5})$ fits the experimental data. Further, we note that if the present $SU(6)$ model is supersymmetrized, then a large enhancement in $\sigma_{\gamma\gamma}$ is possible due to loop contributions from superpartners of vectorlike leptons and quarks. This fact has been previously pointed out by Refs. [21,25]. In Table III, we additionally present a third benchmark (BP-3) that takes into account possible loop contribution from sleptons and squarks. For simplicity, we assume $A_f = M_{\tilde{f}} = M_f$ for this supersymmetrized BP. The inclusion of sparticles improves $\sigma_{\gamma\gamma}$ by a factor of ∼2.34.

We now discuss constraints from a few associated diboson $(S \to W^+W^-, ZZ, Z\gamma)$ final states that arise from the decay widths presented in Eq. (14). The $W^+W^-, ZZ, Z\gamma$ signals are estimated to occur with a rate comparable to that of the $\gamma\gamma$ channel, being that they originate from the same set of couplings. Among these three weak-boson channels, the $Z\gamma$ channel is the most stringent, and ATLAS [26] constrains a monophoton signal to be less than 30 fb at 13 TeV. The two $3 \times (5, \bar{5})$ cases considered here clearly satisfy these bounds.

Next, we focus on the $gg$ channel in some detail, since it takes up a sizeable partial width in comparison to $\gamma\gamma$.

TABLE III. Total decay width of $S$ and cross sections in associated diboson final states for $M_S = 745$ GeV for different BPs belonging to $3 \times (5, \bar{5})$. The choice of values of parameters $M_L$, $M_D$ is also shown, while fixing $\lambda_L = 0.4$ and $\lambda_D = 0.7$. For the minimal supersymmetric standard model (MSSM) BP we choose $A_f = M_{\tilde{f}} = M_f$ $(f = D, L)$ for simplicity. We also included $\alpha_s^4$ correction to $\Gamma_{gg}$, which increases it by a factor of ∼1.7.

| | | $(M_L, M_D)$ (GeV) | $\Gamma_S$ (GeV) | $\sigma_{\gamma\gamma}$ (fb) | $\sigma_{ZZ}$ (fb) | $\sigma_{Z\gamma}$ (fb) | $\sigma_{WW}$ (fb) | $\sigma_{gg}$ (fb) |
|---|---|---|---|---|---|---|---|---|
| SM + $3 \times (5, \bar{5})$ | BP-1 | (374,655) | 0.03 | 2.61 | 5.06 | 0.71 | 13.4 | 437 |
| | BP-2 | (500,875) | 0.02 | 1.00 | 1.82 | 0.22 | 4.73 | 229 |
| MSSM + $3 \times (5, \bar{5})$ | BP-3 | (374,655) | 0.06 | 6.10 | 12.7 | 2.04 | 34.1 | 697 |

CMS places the strongest ∼1.3 pb bound on a 750 GeV $gg$ resonance at 13 TeV [27]. Evidently, our BPs survive the dijet bounds arising from the 13 TeV ATLAS analysis.

Finally, in the case of a supersymmetrized model, we can additionally resolve the narrow-width problem by a possible decay of $S$ into a pair of lightest supersymmetric particles (LSPs) with large width. However, an invisible width sufficiently large to bring our Table III BPs into compatibility with this interpretation is in slight tension with the monojet bounds [21,28]. Such a conflict can easily be avoided by promoting a candidate invisible final state into the "semi-invisible" regime, e.g. by decaying $S$ into a pair of next-to-LSPs (NLSPs), and thereafter allowing the NLSP to decay into the LSP and a relatively soft lepton. This scenario may be realized efficiently via off-shell $Z^*/\tilde{l}^*$ decays associated with a kinematically narrow (10–20 GeV) mass gap between the NLSP and LSP. Alternatively, the soft leptons can also be due to a slepton in between the NLSP and LSP. We refer the reader to Ref. [21] for additional details.

## V. CONCLUSION

Vectorlike quarks and leptons with masses around the TeV scale are potentially beneficial for explaining the resonant diphoton excess observed by CMS and ATLAS. However, this explanation triggers many additional questions, such as whether the new scale is associated with any new symmetry, whether the new vectorlike fermions and the SM fermions belong to anomaly-free representations of any GUT group, and whether the scalar particle responsible for the 750 GeV resonance can be economically associated with the new scale and the new symmetry multiplets housing the vectorlike fermions.

In this paper, we made attempts to answer all of these questions in the context of an $SU(6)$ GUT model. The vectorlike fermions, along with the SM fermions, appear in the smallest anomaly-free $15 + \bar{6} + \bar{6}'$ representations of $SU(6)$, where $SU(6)$ breaks down to the SM $\times\, U(1)_X$ at the GUT scale. Masses for the vectorlike fermions are generated at the TeV scale where $U(1)_X$ is broken by a VEV of the SM singlet field arising from $\bar{6}_H$ and 21. This singlet in the $\bar{6}_H$ field is also responsible in turn for the observed resonance. The dark matter arises from the SM singlet fermion residing in $\bar{6}$s, and is of Majorana type. The SM fermions acquire masses at the electroweak scale.

We additionally demonstrated that a suitable gauge coupling unification is possible in this model, and discussed the Yukawa couplings associated with the vectorlike fields in this model. We also discussed the origin of neutrino masses. The diphoton final states arise due to the three generations of down-type vectorlike quarks and lepton doublets, where $M_L/M_D$ is fixed by a fixed point of the RGEs. We used both 8 and 13 TeV diphoton excess results from ATLAS and from CMS to calculate the masses and couplings associated with the new fields. In addition to the diphoton final states, we also expect $WW$, $WZ$, $ZZ$, and dijet final states. We have carefully studied the final states associated with this model's $SU(6)$ context, arriving at unique predictions that can be used to distinguish it at the LHC.

The 750 GeV diphoton excess has similarly been studied in the context of $U(1)'$ models by several groups, e.g. [29–34], but identification of the unifying $SU(6)$ GUT and the associated particle content render this effort and its predictions different from other works. In the present case, we have considered a nonsupersymmetric $U(1)_X$ model with fermionic vectorlike particles. In contrast with the supersymmetric $U(1)_X$ models, this construction does not suffer from dimension-5 proton decay via exchanges of scalar color triplets. Also, vectorlike masses are forbidden here by the $U(1)_X$ gauge symmetry, and are generated dynamically only after $U(1)_X$ gauge symmetry breaking. In Ref. [29], the supersymmetric $U(1)_N$ model has been studied. To avoid the dimension-5 proton decay problem, the authors imposed a symmetry such as $Z_2^{qq}$ or $Z_2^{lq}$, which could become subtle if one generation forms a complete fundamental representation of $E_6$. Also, the doublets from vectorlike particles are interpreted there as inert. In Ref. [30], vectorlike particle masses are not forbidden by the $U(1)_X$ gauge symmetry, and the model does not have an $E_6/SU(6)$ embedding. Similarly, in Ref. [31], an additional $U(1)_B$ has been considered without any unifying GUT symmetry. In Ref. [32], a supersymmetric $U(1)'$ model has been considered, which again cannot be embedded into $E_6$. Reference [33] deals with a leptophobic $U(1)_X$ in the context of $E_6$. Finally, Ref. [34] analyzed and developed phenomenological tools by comparing all the $U(1)$ extension models proposed in the context of diphoton excess.

## ACKNOWLEDGMENTS

We thank Teruki Kamon and Zurab Tavartkiladze for helpful discussions. This work is supported in part by DOE Award No. DE-FG02-13ER42020 (B. D. and T. G.), the Mitchell Institute for Fundamental Physics and Astronomy (Y. G.), Bartol Research Institute (I. G.), the Rustaveli National Science Foundation Grant No. 03/79 (I. G.), Natural Science Foundation of China Grants No. 11135003, No. 11275246, and No. 11475238 (T. L.), and National Science Foundation Grant No. PHY-1521105 (J. W. W.).

## APPENDIX A: $SU(3)_C \times SU(2)_L \times U(1)_Y \times U(1)_X$ MODEL OF $SU(6)$ FROM $E_6$ EMBEDDING

$E_6$ has a subgroup $SU(6) \times SU(2)$, and the fundamental representation of $E_6$ decomposes as

$$\mathbf{27} \to (\bar{\mathbf{6}}, \mathbf{2}) \oplus (\mathbf{15}, \mathbf{1}). \tag{A1}$$

TABLE IV. Decomposition of the $E_6$ fundamental **27** representation under $SO(10)$ and $SU(5)$, and the $U(1)_\chi$, $U(1)_\psi$, and $U(1)'$ charges.

| $SO(10)$ | $SU(5)$ | $2\sqrt{10}Q_\chi$ | $2\sqrt{6}Q_\psi$ | $2\sqrt{15}Q'$ |
|---|---|---|---|---|
| | **10** | −1 | 1 | 2 |
| 16 | $\bar{\mathbf{5}}$ | 3 | 1 | −1 |
| | **1** | −5 | 1 | 5 |
| | **5** | 2 | −2 | −4 |
| 10 | $\bar{\mathbf{5}}$ | −2 | −2 | −1 |
| 1 | **1** | 0 | 4 | 5 |

Thus, our $SU(3)_C \times SU(2)_L \times U(1)_Y \times U(1)_X$ model from $SU(6)$ can be embedded into $E_6$. We consider $SU(6) \to SU(5) \times U(1)_X$. And the generator of $U(1)_X$ is $T_{U(1)_X} = \frac{1}{2\sqrt{15}}\text{diag}(1, 1, 1, 1, 1, -5)$. Thus, we obtain

$$\mathbf{15} \to (\overline{\mathbf{10}}, \mathbf{2}) \oplus (\mathbf{5}, -\mathbf{4}), \tag{A2}$$

$$\bar{\mathbf{6}} \to (\bar{\mathbf{5}}, -\mathbf{1}) \oplus (\mathbf{1}, \mathbf{5}), \tag{A3}$$

where the above $U(1)_X$ quantum numbers are $2\sqrt{15}Q_X$. In other words, the correct $U(1)_X$ charges are the above $U(1)_X$ charges divided by $2\sqrt{15}$.

The $E_6$ gauge group can be broken as follows [35,36]. $E_6 \to SO(10) \times U(1)_\psi \to SU(5) \times U(1)_\chi \times U(1)_\psi$. The $U(1)_\psi$ and $U(1)_\chi$ charges for the $E_6$ fundamental **27** representation are given in Table IV. The $U(1)'$ is one linear combination of the $U(1)_\chi$ and $U(1)_\psi$, $Q' = \cos\theta Q_\chi + \sin\theta Q_\psi$. For simplicity, we assume that the other $U(1)$ gauge symmetry from the orthogonal linear combination of the $U(1)_\chi$ and $U(1)_\psi$ is absent or broken at a high scale. For the fundamental representation **27** decomposition, see Table IV.

To realize the $U(1)_X$ gauge symmetry of $SU(6)$, we require that two singlets in Table IV have the same $U(1)'$ charges. Thus, we obtain $\cos\theta = -\sqrt{\frac{3}{8}}$. We present the $U(1)'$ charges in Table IV, and the $U(1)'$ charges are indeed the same as our $U(1)_X$ charges. Such kinds of $U(1)'$ models have been studied before [37–43]. In particular, the $U(1)'$ gauge symmetry in Ref. [39] is the same as our $U(1)_X$ gauge symmetry from $SU(6)$, up to the overall sign difference for the charges. However, in Ref. [39], the authors did not embed the $U(1)'$ model into an $E_6$ model explicitly, and the gauge symmetry breaking $E_6 \to SU(3)_C \times SU(2)_L \times U(1)_Y \times U(1)'$ may be nontrivial.

## APPENDIX B: RENORMALIZATION GROUP EVOLUTION

The relevant structure of the $SU(3)_C \times SU(2)_L \times U(1)_Y \times U(1)_X$ nonsupersymmetric renormalization group evolution is subsequently recapped. We work to the second loop in the gauge couplings $\alpha_i \equiv g_i^2/4\pi$ $(i \equiv Y, 2, 3, X)$, and to the first loop for the Yukawa couplings $\varkappa_f \equiv |\lambda_f|^2/4\pi$ $(f \equiv t, b, \tau)$, truncating consideration to the third generation. Derivatives are taken with respect to $t = \ln(\mu/\mu_0)$, the logarithm of the renormalization scale.

$$\frac{d\alpha_i}{dt} = \frac{b_i\alpha_i^2}{2\pi} + \frac{\alpha_i^2}{8\pi^2}\left[\sum_{j=1}^{3} B_{ij}\alpha_j - \sum_{\tilde{f}=t,b,\tau} C_{i\tilde{f}}\varkappa_{\tilde{f}}\right] \tag{B1}$$

$$\left.\frac{d\varkappa_f}{dt}\right|_{[t,b,\tau]} = \frac{\varkappa_f}{2\pi}\left[\sum_{\tilde{f}=t,b,\tau} Y_{f\tilde{f}}\varkappa_{\tilde{f}} - \sum_{j=1}^{3} D_{fj}\alpha_j\right]. \tag{B2}$$

The $\beta$-coefficients associated with the standard model field content, including a single Higgs doublet, are shown following. We include the fourth ($X$) index in the tabulation of the gauge sector coefficients ($b_i$ and $B_{ij}$), consistent with the assignment of quantum numbers described in Appendix A. Although the $U(1)_X$ symmetry is actually hypothesized to be broken around the TeV scale, we continue the running of $\alpha_X$ down to $M_Z$ for simplicity (with negligible effect due to the weakness of that coupling in this regime), as in Fig. 1. We neglect coupling to $\alpha_X$ in the Yukawa sector.

$$b = \begin{pmatrix} \frac{41}{10} \\ \frac{19}{6} \\ -7 \\ \frac{361}{90} \end{pmatrix} \qquad B = \begin{pmatrix} \frac{199}{50} & \frac{27}{10} & \frac{44}{5} & \frac{71}{50} \\ \frac{9}{10} & \frac{35}{6} & 12 & \frac{43}{30} \\ \frac{11}{10} & \frac{9}{2} & -26 & \frac{7}{5} \\ \frac{71}{50} & \frac{43}{10} & \frac{56}{5} & \frac{1081}{450} \end{pmatrix} \tag{B3}$$

$$C = \begin{pmatrix} \frac{17}{10} & \frac{1}{2} & \frac{3}{2} \\ \frac{3}{2} & \frac{3}{2} & \frac{1}{2} \\ 2 & 2 & 0 \end{pmatrix} \quad Y = \begin{pmatrix} \frac{9}{2} & \frac{3}{2} & 1 \\ \frac{3}{2} & \frac{9}{2} & 1 \\ 3 & 3 & \frac{5}{2} \end{pmatrix} \quad D = \begin{pmatrix} \frac{17}{20} & \frac{9}{4} & 8 \\ \frac{1}{4} & \frac{9}{4} & 8 \\ \frac{9}{4} & \frac{9}{4} & 0 \end{pmatrix}. \tag{B4}$$

Low-energy boundary values of the SM gauge couplings are defined in the usual manner,

$$\alpha_Y = \frac{5\alpha_{em}(M_Z)}{3(1-\sin^2\theta_W)} \quad \alpha_2 = \frac{\alpha_{em}(M_Z)}{\sin^2\theta_W} \quad \alpha_3 \equiv \alpha_s(M_Z), \tag{B5}$$

using the following precision electroweak inputs:

$$\alpha_{em}(M_Z) = \frac{1}{127.94} \qquad \alpha_s(M_Z) = .1185$$
$$\sin^2\theta_W^{\overline{MS}}(M_Z) = .23126 \qquad M_Z = 91.1876\ [\text{GeV}]. \tag{B6}$$

The coupling $\alpha_X$, which has no corresponding electroweak value, is instead constrained to unify at the high scale boundary and subsequently run down. The low-energy boundary values of the top and bottom quark Yukawa couplings are expressed in terms of the experimentally

measured Fermi coupling $G_{\rm F} = 1.16638 \times 10^{-5}$ [GeV$^{-2}$]$\equiv \{2\sqrt{2}(v_u^2 + v_d^2)\}^{-1}$, the ratio $\tan\beta \equiv (v_u/v_d)$ of the up- and downlike Higgs VEVs, and the relevant pole masses. For concreteness, we take $\tan\beta = 10$.

$$m_t \equiv \lambda_t v_u = 173.3 \text{ [GeV]} \qquad m_b \equiv \lambda_b v_d = 4.18 \text{ [GeV]}$$
$$m_\tau \equiv \lambda_\tau v_d = 1.777 \text{ [GeV]} \tag{B7}$$

$$\varkappa_t = \frac{m_t^2 G_F}{\pi\sqrt{2}}\left(1 + \frac{1}{\tan^2\beta}\right) \qquad \varkappa_{b,\tau} = \frac{m_{b,\tau}^2 G_F}{\pi\sqrt{2}}(1 + \tan^2\beta). \tag{B8}$$

Threshold modifications to renormalization of the gauge sector in the first and second loop attributable to field content beyond the standard model are as follows, where indices $I$, $II$ respectively denote the field content active around the TeV scale, and above the intermediate ($\sim 10^{10}$ GeV) scale, as described in Sec. III:

$$\delta b^I = \begin{pmatrix} \frac{21}{10} \\ \frac{13}{6} \\ 2 \\ \frac{487}{180} \end{pmatrix} \qquad \delta B^I = \begin{pmatrix} \frac{22}{25} & \frac{18}{5} & \frac{16}{5} & \frac{3}{25} \\ \frac{6}{5} & \frac{80}{3} & 0 & \frac{2}{15} \\ \frac{2}{5} & 0 & 38 & \frac{1}{10} \\ \frac{3}{25} & \frac{2}{5} & \frac{4}{5} & \frac{12517}{900} \end{pmatrix} \tag{B9}$$

$$\delta b^{II} = \begin{pmatrix} 0 \\ \frac{8}{3} \\ 2 \\ 0 \end{pmatrix} \qquad \delta B^{II} = \begin{pmatrix} 0 & 0 & 0 & 0 \\ 0 & \frac{176}{3} & 0 & 0 \\ 0 & 0 & 84 & 0 \\ 0 & 0 & 0 & 0 \end{pmatrix}. \tag{B10}$$

Additionally, we consider running under the renormalization group of the Yukawa couplings $(\lambda_L, \lambda_D)$ between the lepton-doubletlike and down-quarklike components of the vectorlike $3 \times (5, \bar{5})$ and the SM singlet $\bar{6}'_H$. We define $\varkappa_i \equiv \lambda_i^2/4\pi$, with $i = (1\ldots6)$, where indices $(1\ldots3)$ reference the $\lambda_L$ and indices $(4\ldots6)$ reference the $\lambda_D$. The associated renormalization group equations and $\beta$-function matrices are as follows:

$$\frac{d\varkappa_i}{dt} = \frac{\varkappa_i}{2\pi}\left[\sum_{j=1}^{6} \mathcal{Y}_{ij}\varkappa_j - \sum_{j=1}^{3} \mathcal{D}_{ij}\alpha_j\right] \tag{B11}$$

$$\mathcal{Y} = \begin{pmatrix} \frac{7}{2} & 2 & 2 & 3 & 3 & 3 \\ 2 & \frac{7}{2} & 2 & 3 & 3 & 3 \\ 2 & 2 & \frac{7}{2} & 3 & 3 & 3 \\ 2 & 2 & 2 & \frac{9}{2} & 3 & 3 \\ 2 & 2 & 2 & 3 & \frac{9}{2} & 3 \\ 2 & 2 & 2 & 3 & 3 & \frac{9}{2} \end{pmatrix} \qquad \mathcal{D} = \begin{pmatrix} \frac{9}{10} & \frac{9}{2} & 0 \\ \frac{9}{10} & \frac{9}{2} & 0 \\ \frac{9}{10} & \frac{9}{2} & 0 \\ \frac{4}{5} & 0 & 8 \\ \frac{4}{5} & 0 & 8 \\ \frac{4}{5} & 0 & 8 \end{pmatrix}. \tag{B12}$$

A strong quasifixed point attraction in the infrared is observed for the $\lambda$s. This behavior is analogous to that observed by Pendleton and Ross [44] for the top quark Yukawa coupling, wherein attraction toward an approximately universal value is observed at low energy when starting from a sufficiently large coupling at the GUT-scale boundary. This effect is attributable to shepherding by the strong coupling $\alpha_s$, enforced via cancellation between the gauge and Yukawa contributions to the right-hand side of Eq. (B11). There is no universal behavior for weak coupling at the GUT scale, which generically also results in weaker coupling at low energy. Specifically, the described attraction favors coupling values in the vicinity of $\lambda_L = 0.4$ and $\lambda_D = 0.7$ at the scale of the diphoton resonance.


[1] The ATLAS Collaboration, Report No. ATLAS-CONF-2015-081, 2015.
[2] CMS Collaboration, Report No. CMS-PAS-EXO-15-004, 2015.
[3] The ATLAS Collaboration, Report No. ATLAS-CONF-2016-018, 2015.
[4] CMS Collaboration, Report No. CMS-PAS-EXO-16-018, 2015.
[5] R. Franceschini, G. F. Giudice, J. F. Kamenik, M. McCullough, A. Pomarol, R. Rattazzi, M. Redi, F. Riva, A. Strumia, and R. Torre, J. High Energy Phys. 03 (2016) 144.
[6] S. Knapen, T. Melia, M. Papucci, and K. Zurek, Phys. Rev. D **93**, 075020 (2016).
[7] K. Harigaya and Y. Nomura, Phys. Lett. B **754**, 151 (2016); M. Backovic, A. Mariotti, and D. Redigolo, J. High Energy Phys. 03 (2016) 157; A. Angelescu, A. Djouadi, and G. Moreau, Phys. Lett. B **756**, 126 (2016); Y. Nakai, R. Sato, and K. Tobioka, Phys. Rev. Lett. **116**, 151802 (2016); S. Knapen, T. Melia, M. Papucci, and K. Zurek, Phys. Rev. D **93**, 075020 (2016); D. Buttazzo, A. Greljo, and D. Marzocca, Eur. Phys. J. C **76**, 116 (2016); A. Pilaftsis, Phys. Rev. D **93**, 015017 (2016); S. D. McDermott, P. Meade, and H. Ramani, Phys. Lett. B **755**, 353 (2016); A. Kobakhidze, F. Wang, L. Wu, J. M. Yang, and M. Zhang, Phys. Lett. B **757**, 92 (2016); S. Fichet, G. von Gersdorff, and C. Royon, Phys. Rev. D **93**, 075031 (2016); B. Dutta, Y. Gao, T. Ghosh, I. Gogoladze, and T. Li, Phys. Rev. D **93**, 055032 (2016); P. S. B. Dev, R. N. Mohapatra, and Y. Zhang, J. High Energy Phys. 02 (2016) 186; G. M. Pelaggi, A. Strumia, and E. Vigiani, J. High Energy Phys. 03 (2016)

025; S. Di Chiara, L. Marzola, and M. Raidal, Phys. Rev. D **93**, 095018 (2016).
[8] I. Gogoladze, B. He, and Q. Shafi, Phys. Lett. B **690**, 495 (2010).
[9] P. Minkowski, Phys. Lett. **67B**, 421 (1977); T. Yanagida, *Workshop on Unified Theories* (KEK Report 79–18, Tsukuba, 1979), p. 95; M. Gell-Mann, P. Ramond, and R. Slansky, *Supergravity* (Amsterdam, North Holland, 1979), p. 315; S. L. Glashow, *1979 Cargese Summer Institute on Quarks and Leptons* (Plenum, New York, 1980), p. 687; R. N. Mohapatra and G. Senjanovic, Phys. Rev. Lett. **44**, 912 (1980).
[10] See for instance Q. Shafi and Z. Tavartkiladze, Phys. Lett. B **522**, 102 (2001) and references threrein.
[11] F. del Aguila, J. de Blas, and M. Perez-Victoria, Phys. Rev. D **78**, 013010 (2008); A. Freitas, J. Lykken, S. Kell, and S. Westhoff, J. High Energy Phys. 05 (2014) 145; 09 (2014) 155(E).
[12] G. W. Bennett *et al.* (Muon g-2 Collaboration), Phys. Rev. D **73**, 072003 (2006).
[13] P. A. R. Ade *et al.* (Planck Collaboration), Astron. Astrophys. **571**, A16 (2014); A. G. Riess *et al.*, Astrophys. J. **826**, 56 (2016).
[14] R. Slansky, Phys. Rep. **79**, 1 (1981).
[15] E. Ma, Phys. Rev. D **88**, 117702 (2013).
[16] B. Dutta, Y. Gao, T. Ghosh, I. Gogoladze, T. Li, and J. W. Walker (to be published).
[17] U. Amaldi, W. de Boer, P. H. Frampton, H. Furstenau, and J. T. Liu, Phys. Lett. B **281**, 374 (1992).
[18] J. L. Chkareuli, I. G. Gogoladze, and A. B. Kobakhidze, Phys. Lett. B **340**, 63 (1994).
[19] The ATLAS Collaboration, https://atlas.web.cern.ch/Atlas/GROUPS/PHYSICS/CombinedSummaryPlots/EXOTICS/index.html#ATLAS_Exotics_Summary.
[20] V. Khachatryan *et al.* (CMS Collaboration), J. High Energy Phys. 03 (2016) 125.
[21] B. Dutta, Y. Gao, T. Ghosh, I. Gogoladze, T. Li, Q. Shafi, and J. W. Walker, arXiv:1601.00866.
[22] A. D. Martin, W. J. Stirling, R. S. Thorne, and G. Watt, Eur. Phys. J. C **63**, 189 (2009).
[23] S. Catani, D. de Florian, M. Grazzini, and P. Nason, J. High Energy Phys. 07 (2003) 028.
[24] K. G. Chetyrkin, B. A. Kniehl, and M. Steinhauser, Phys. Rev. Lett. **79**, 353 (1997).
[25] H. P. Nilles and M. W. Winkler, J. High Energy Phys. 05 (2016) 182.
[26] The ATLAS Collaboration, Report No. ATLAS-CONF-2016-010, 2016.
[27] The ATLAS Collaboration, Report No. ATLAS-CONF-2016-030, 2016.
[28] A. Falkowski, O. Slone, and T. Volansky, J. High Energy Phys. 02 (2016) 152.
[29] S. F. King and R. Nevzorov, J. High Energy Phys. 03 (2016) 139.
[30] K. Das and S. K. Rai, Phys. Rev. D **93**, 095007 (2016).
[31] M. Duerr, P. F. Perez, and J. Smirnov, arXiv:1604.05319.
[32] Y. Jiang, Y. Y. Li, and T. Liu, Phys. Lett. B **759**, 354 (2016).
[33] P. Ko, Y. Omura, and C. Yu, J. High Energy Phys. 04 (2016) 098.
[34] F. Staub *et al.*, arXiv:1602.05581.
[35] R. Slansky, Phys. Rep. **79**, 1 (1981).
[36] J. L. Hewett and T. G. Rizzo, Phys. Rep. **183**, 193 (1989).
[37] For a review, see P. Langacker, Rev. Mod. Phys. **81**, 1199 (2009).
[38] J. Erler, Nucl. Phys. **B586**, 73 (2000).
[39] P. Langacker and J. Wang, Phys. Rev. D **58**, 115010 (1998).
[40] J. Erler, P. Langacker, and T. Li, Phys. Rev. D **66**, 015002 (2002).
[41] J. Kang, P. Langacker, T. Li, and T. Liu, Phys. Rev. Lett. **94**, 061801 (2005).
[42] J. h. Kang, P. Langacker, and T. Li, Phys. Rev. D **71**, 015012 (2005).
[43] J. Kang, P. Langacker, T. Li, and T. Liu, J. High Energy Phys. 04 (2011) 097.
[44] B. Pendleton and G. G. Ross, Phys. Lett. **98B**, 291 (1981).